Published in final edited form as:
Biomaterials. 2014 October ; 35(31): 8846–8853. doi:10.1016/j.biomaterials.2014.07.003.

A composite hydrogel platform for the dissection of tumor cell migration at tissue interfaces

Andrew Rape and **Sanjay Kumar**[1]
Department of Bioengineering, University of California, Berkeley

Abstract

Glioblastoma multiforme (GBM), the most prevalent primary brain cancer, is characterized by diffuse infiltration of tumor cells into brain tissue, which severely complicates surgical resection and contributes to tumor recurrence. The most rapid mode of tissue infiltration occurs along blood vessels or white matter tracts, which represent topological interfaces thought to serve as “tracks” that speed cell migration. Despite this observation, the field lacks experimental paradigms that capture key features of these tissue interfaces and allow reductionist dissection of mechanisms of this interfacial motility. To address this need, we developed a culture system in which tumor cells are sandwiched between a ventral fibronectin-coated dorsal surface representing vascular basement membrane and a dorsal hyaluronic acid (HA) surface representing brain parenchyma. We find that inclusion of the dorsal HA surface induces formation of adhesive complexes and significantly slows cell migration relative to a free fibronectin-coated surface. This retardation is amplified by inclusion of integrin binding peptides in the dorsal layer and expression of CD44, suggesting that the dorsal surface slows migration through biochemically specific mechanisms rather than simple steric hindrance. Moreover, both the reduction in migration speed and assembly of dorsal adhesions depend on myosin activation and the stiffness of the ventral layer, implying that mechanochemical feedback directed by the ventral layer can influence adhesive signaling at the dorsal surface.

Introduction

Cell migration and the mechanisms that underlie specific migratory phenotypes are increasingly recognized to depend on extracellular context, especially the structure and mechanics of the extracellular matrix (ECM) [1–3]. On planar two-dimensional substrates, migration is typically described as being driven by a balance between actin polymerization at the cell front and actomyosin contraction at the cell rear that are transmitted to the ECM via adhesions [4]. In three-dimensional ECMs, migration can take various forms including

[1]Author for correspondence: Sanjay Kumar; 274A Stanley Hall #1762; University of California, Berkeley; Berkeley, CA 94720 (skumar@berkeley.edu).

The authors do not disclose any conflicts of interest.

mesenchymal migration (perhaps most analogous to classical two-dimensional migration) to amoeboid migration, which is less adhesion-dependent and leverages intracellular hydrostatic pressure generated by actomyosin contractility to extrude the cell body through matrix pores [5]. Importantly, the molecular mechanisms that control these migration modes are as diverse as the number of migratory phenotypes. In fact, many cells dynamically switch from one mode to another as they encounter and navigate different microenvironments, highlighting the importance of studying cell migration in culture systems that capture defining architectural features of tissue [6–8].

Cell migration is often guided by heterogeneous structures within the ECM; for example, a diverse variety of invasive solid tumors proceed along pre-existing anatomical structures [9–12]. Metastastatic tumor cells have been clinically observed to preferentially migrate in bone cavities or between adipocytes, suggesting that the topographies of these structures may facilitate tissue dissemination [10]. Migration in this context may be regarded as being “interfacial” in nature, in that cells translocate along a ventral two-dimensional surface while surrounded on their dorsolateral surface by an amorphous ECM of a different composition. Other examples of interfacial migration are tumor cells that migrate between bundles of myelinated axons and connective brain tissue [10,13].

A particularly important example of interfacial migration is the invasion of glioblastoma multiforme (GBM), the most common and deadly primary brain tumor. The extreme lethality of this malignancy is attributed in part to its diffuse and unrelenting infiltration of the brain parenchyma, effectively precluding complete surgical resection [14]. GBM invasion patterns are unlike most other aggressive malignancies, in that GBM cells rarely intravasate and metastasize to distant tissues, instead remaining within the brain [14,15]. The pre-existing structures that guide GBM, collectively known as the secondary structures of Scherer, include the subpial space, white matter tracts, and vascular beds [16]. While these structures are widely acknowledged to facilitate invasive migration, relatively little is known about the biophysical and molecular mechanisms through which they do so. For example, cells migrating along vascular beds simultaneously experience strong integrin-based inputs via fibronectin and laminin in the vascular basement membrane [15] while also receiving adhesive inputs from hyaluronic acid in the brain parenchyma, which can be mediated by HA receptors such as CD44 and RHAMM [17,18]. There are also substantial biophysical asymmetries within this adhesive microenvironment, as vascular beds tend to be orders of magnitude stiffer than the surrounding parenchyma [19–21]. How these asymmetric signals are integrated to regulate migration in GBM remains unknown.

Despite the acknowledged importance of migration along asymmetric tissue interfaces in many tumors, comparatively little is known about the molecular mechanisms that underlie this process. The fact that migration mechanisms depend strongly on context has created an unmet need for experimental paradigms that recapitulate key aspects of these interfaces. To address this need, we developed a simple experimental system that features asymmetric ECM signals representative of the brain parenchyma-vascular interface, and used it to investigate molecular mechanisms of adhesion and motility.

Methods

HA-methacrylate synthesis

Methacrylated HA was synthesized as described previously [22]. Briefly, high molecular weight HA (66kDa-90kDa; Lifecore technologies) was dissolved at 1 wt% in deionized water, and then a six-fold molar excess of methacrylic anhydride (Sigma) was added dropwise to the solution on ice. The pH of the reaction was adjusted to a value greater than 8, where it was held for the duration of the experiment. The reaction was allowed to proceed overnight. HA-methacrylate was isolated by the addition of a five-fold volumetric excess of cold acetone to the reaction solution. This mixture was then centrifuged to recover the precipitate, which contained the HA-methacrylate. The precipitate was then dissolved in water, flash-frozen, and lyophilized.

Interfacial culture system formation

Initially, fibronectin-coated polyacrylamide surfaces were prepared as described previously [23]. After sterilization of the hydrogels, U373-MG, U87-MG, or U373-MGU cells were plated on the gels and allowed to adhere overnight. 25 μl of an HA-methacrylate solution was then poured onto the cell and crosslinked in situ with the bifunctional dithiothreitol (DTT; Sigma) to form covalent cross-links among HA chains [24]. In HA-RGD formulations, cysteine containing RGD peptide (Ac-GCGYGRDSPG-NH2; Anaspec) was first reacted with HA-methacrylate for 2 hours, prior to gelation. All hydrogels consisted of 5 wt% HA-methacryate. The solution was immediately sandwiched with a glass coverslip and allowed to polymerize for 4 hours at 37C, after which fresh medium was added.

Cell culture

U373-MG and U87-MG human glioblastoma cells were obtained from the University of California, Berkeley Tissue Culture facility and cultured as described previously [23] in DMEM (Invitrogen) supplemented with 10% Calf Serum Advantage (JR Scientific, Inc.), 1% penicillin-streptomycin, 1% MEM non-essential amino acids, and 1% sodium pyruvate (Invitrogen). Given the recent recognition that U373-MG likely share an origin with U251-MG cells [25], we also obtained early-passage U373-MG cells (Sigma), which we termed U373-MG-U, reflecting their derivation from the original University of Uppsala stocks [25].

Inhibition of cell contractility

Rho-associated kinase (ROCK) inhibitor Y-27632 (10 μM; Calbiochem), NMMII inhibitor blebbistatin (10 μM; Sigma), or myosin light chain kinase inhibitor (MLCK) ML-7 (1 μM; Calbiochem) was added to cells in interface culture after overnight incubation. Cells were incubated with the drug for at least 12 hours prior to imaging.

Measurement of cell motility

Live-cell imaging was performed with a Nikon TE2000E2 microscope equipped with an incubator chamber for control of temperature, humidity, and carbon dioxide. After formation of the interfacial culture system as described above, phase-contrast images of cells were collected for at least five hours with a 10× objective. Nuclei were then tracked from one

frame to another to yield instantaneous migration speeds, which were then averaged over the entire time course of the experiment to yield the migration speed of a cell.

Fluorescence microscopy

Mouse anti-vinculin primary antibody (Sigma) and AlexaFluor 546 goat anti-mouse secondary antibody (Molecular Probes) were used to visualize vinculin. Rat anti-CD44 primary antibody (Hermes-1, Pierce) and AlexaFluor 647 chicken anti-rat secondary antibody (Molecular Probes) were used to visualize CD44. Nuclei were labeled with 4',6-diamidino-2-phenylindole (DAPI, Invitrogen). To overcome the diffusion limitations imposed by the small pores of the HA overlay, prior to immunostaining but after cell fixation, the HA overlay was digested by treatment with 300 μg/ml hyaluronidase (Sigma) for one hour. Three-dimensional confocal stacks were acquired on a swept-field upright confocal microscope equipped with a 60× water-immersion lens (Prairie Technologies).

Centrifugation assay

After a specified adhesion time, hydrogels were submerged in fresh serum-free media, and the cell culture plate was sealed with adhesive plate sealers. The plate was then inverted and centrifuged for 5 min at 100 g [26]. Cells remaining on the hydrogels were then fixed and stained with DAPI and manually counted using a 40× lens on a Nikon TE2000E2 microscope.

Data analysis and statistics

Statistical significance was tested using ANOVA followed by Tukey-Kramer multiple comparison, and represented by bar plots with error bars representing standard error. Significance level was set at 0.05.

Results

Modeling perivascular migration with interfacial hydrogels

As described earlier, vascular structures are an important secondary Structure of Scherer along which GBM cells invade brain tissue. To model this process in culture, we developed an *in vitro* overlay culture system that recapitulates key features of the matrix environment found at this interface and allows for systematic and independent control of the biophysical and biochemical properties of each matrix (Figure 1A). To mimic the fibronectin-rich basolateral membrane of the vasculature, we used polyacrylamide hydrogels tuned to a stiffness of 119 kPa, consistent with measured stiffness values of vascular beds, and covalently modified with fibronectin, which is strongly enriched in vascular basement membranes [27]. To mimic the HA-rich brain ECM, we used a hyaluronic acid hydrogel that can be cross-linked as a matrix "overlay" in the presence of cells over a wide range of stiffnesses and also can be functionalized with peptide adhesive ligands [22,24,28]. Combining these hydrogels into an overlay-like configuration provides a customizable platform to recreate the interfaces present at the blood vessel-brain barrier upon which GBM tumors preferentially migrate.

Effects of dorsal adhesion on cell migration

We first investigated the interaction between cells and the HA overlay and its contribution to cell migration speed. In these experiments, we cultured cells on polyacrylamide gels as described above and then sandwiched the cells in an interfacial configuration by pouring an HA solution on the dorsal surface and crosslinking the HA in situ with DTT. We then allowed cells to randomly migrate and automatically tracked them with phase contrast microscopy over a 5 hour period. We found that the presence of a HA overlay retarded the migration speed of U373-MG human glioma cells approximately twofold relative to a control configuration lacking an overlay, (Figure 1B–F). This finding was reproducible across multiple culture models of GBM, as both U87-MG and U373-MG-U cells showed a similar overlay-induced retardation of migration (Figure S1).

Cells engage HA through a variety of adhesive receptors, including CD44, which has been functionally implicated in tumor progression [29,30]. To determine if cells form CD44-positive adhesions at their dorsal surface when presented with an HA overlay, we performed immunofluorescence staining and confocal sectioning. To minimize artifacts associated with antibody retention within the three-dimensional HA gel, we lightly degraded the HA overlay with hyaluronidase after fixation of the cells but prior to antibody incubation. U373-MG cells in the overlay configuration lacked prominent, vinculin-positive focal adhesions on their ventral surface adjacent to the polyacrylamide surface and displayed diffuse CD44-rich adhesions evenly spread along the dorsal surface, indicating that the presence of the dorsal HA layer may retard the ability of these cells to form strong focal adhesions on the opposite adhesive plane (Figure 2).

Role of CD44 in interfacial migration

To determine whether these dorsal HA-CD44 adhesions contribute functionally to cell migration, we depleted CD44 by stably transducing U373-MG cells with a CD44-directed shRNA, which reduced CD44 protein levels to ~60% relative to cells transduced with a non-specific shRNA [26]. When cultured on two-dimensional polyacrylamide-fibronectin surfaces without an overlay, CD44 knockdown (CD44KD) cells were morphologically indistinguishable from naïve and control shRNA-transduced cells cultured on the same surfaces, spreading extensively and forming broad lamellipodia. Similarly, migration speeds of control and CD44KD cells on unconfined fibronectin-coated substrates were statistically indistinguishable, consistent with the absence of HA on these ventral surfaces. However, when cultured in the overlay configuration, the CD44KD cells migrated at speeds nearly 40% faster than control cells, albeit still more slowly than cells with no overlay (Figure 3A).

Given that dorsal HA-CD44 interactions are necessary for maximal retardation of motility, we next investigated the biochemical and biophysical components of this effect. To ask whether HA receptor ligation per se is sufficient to slow migration, independent of the physical context in which that ligation occurs, we cultured U373-MG cells on polyacrylamide-fibronectin gels and treated them with soluble (i.e. non-crosslinked), unmodified high molecular weight HA, which has been previously demonstrated to bind and activate CD44 [24]. Unlike our observation with an HA gel overlay, soluble HA slightly increased the migration speed of U373-MG cells (Figure 3B), indicating that HA receptor

engagement alone is insufficient to slow migration and that it must be anchored within a solid-state matrix.

Role of dorsal adhesion through other receptor-ligand interactions

Given that the brain parenchyma also contains ligands that activate other cell surface receptors, such as the ligation of integrins by an RGD-like domain on tenascin, we next wanted to investigate whether the previously discovered phenomenon was specific to CD44 [31,32]. To determine whether dorsal adhesion-mediated retardation of migration is HA-CD44 specific or a more general property of dorsal adhesion, we further increased the adhesivity of the dorsal surface by conjugating cysteine-containing RGD peptides to the dorsal HA gel backbone using Michael addition chemistry. Cells sandwiched with an HA-RGD overlay displayed an elongated, spindle-shaped morphology devoid of broad lamellipodia, consistent with a previous report in which cells were sandwiched between two fibronectin coated polyacrylamide hydrogels (Figure 4B) [33]. Moreover, the presence of the dorsal RGD peptides slowed migration of WT and CD44KD cells to similar levels, suggesting that this dorsal adhesion-mediated migration retardation is a general phenomenon of both CD44- and integrin-based ligation (Figure 4C).

Effects of myosin II on dorsal adhesion

Myosin-based cell contractility plays a central role in reinforcement of adhesions formed on 2D matrix substrates [34,35] and, as mentioned earlier, figures centrally in facilitating various forms of 3D motility [6]. We therefore wondered whether myosin-dependent contractility might also regulate migration in this overlay paradigm. We pharmacologically inhibited myosin activity with blebbistatin in both the overlay and unconfined configurations and measured effects on cell motility. At sufficiently low dose (10 μM), blebbistatin had only a very modest effect on migration on unconfined migration (Figure S2), consistent with previous reports [3]. In the overlay configuration, however, myosin II inhibition increased migration speed when a bare HA overlay was employed (Figure 5A). When we repeated this study with an HA-RGD overlay, we found that myosin inhibition increased migration speed relative to drug-free controls, but did not restore migration speed to levels observed with a bare HA overlay. This reflects the possibility that at this dosage, blebbistatin may reduce focal adhesion size but not completely abrogate focal adhesion formation or tension generation (Figure 5B) [36]. We observed similar but more muted effects in the setting of ROCK and MLCK inhibition (Y-27632 and ML-7, respectively), further supporting the dependence of this effect on myosin contractility.

These results suggest that myosin II inhibition may strengthen dorsal adhesions, which in turn causes retardation of migration speed. One would therefore predict that ECM conditions that suppress myosin II activation would reduce the restrictive effects of dorsal adhesions. To test this hypothesis, we varied the stiffness of the polyacrylamide layer, which has been shown previously to alter myosin activation and cell contractility, with stiffer gels producing greater myosin activation [37–40]. Based on this hypothesis, we would expect high polyacrylamide stiffness to amplify the anti-motility effects of the HA overlay and produce a greater reduction in migration speed. Indeed, when cultured on stiff polyacrylamide gels and covered with an HA overlay, the migration speed of U373-MG control cells fell by 47%

relative to migration on a unconfined hydrogel of the same stiffness (Figure 6A, B). However, when a soft polyacrylamide gel was used, we observed only a 34% reduction in migration speed. CD44KD cells showed a similar trend, with migration speed falling 23% on stiff polyacrylamide ECMs and remaining unchanged on soft ECMs (Figure 6C, D).

Interactions between CD44, integrins, and myosin II

To more directly test the hypothesis that myosin strengthens adhesion to the dorsal overlay, we used a centrifiguation assay that measures the adhesive strength between cells and the ECM [26]. Briefly, a defined number of cells was cultured on top of a bare HA or RGD-HA hydrogel and allowed to adhere overnight. The gels were then centrifuged to dislodge loosely adhered cells, and then the remaining cells were counted as a readout of cell adhesive strength. We found that pharmacological inhibition of myosin, ROCK, and MLCK all significantly reduced adhesion to both bare HA and HA-RGD surfaces (Figure 7A), consistent with the idea that contractility strengthens CD44-HA adhesion. These results support the notion that strong dorsal adhesion reduces migration speed, whatever the specific nature of that adhesion. To quantitatively explore this, we plotted migration speed against normalized adhesion strength across all of these conditions, which indeed revealed a broad negative correlation between migration speed and dorsal adhesive strength (Figure 7B).

Discussion

Much previous research has illustrated the importance of studying cell migration in a context that recapitulates critical biochemical and biophysical features of the corresponding tissue microenvironment. In this study, we created a simple, reproducible system that allowed us to systematically modulate the asymmetric biophysical and biochemical properties of the dorsal and ventral surfaces of a model tissue interface. This interface could be tailored to include features of the vascular basement membrane-parenchymal space that often guides GBM migration in vivo. Using this system, we found that dorsal adhesion, whether mediated by CD44- or integrin-based adhesions, slows migration in overlay configurations. This paradigm has therefore yielded important new insights into the molecular mechanisms that influence cell migration through heterogeneous tissue interfaces.

When the dorsal region of the cell is engaged with HA, cells migrate with a morphology reminiscent of that on two-dimensional surfaces, with broad leading-edge lamellelipodia that continuously advance. However, when engaged with HA-RGD, cells acquire a spindle-like morphology, as previously observed when cells have been sandwiched a ventral surface and a dorsal surface bearing integrin ligands [33]. Interestingly, we find that dorsal adhesion could slow cell migration through multiple adhesive receptor systems and across a diversity of cell morphologies. Given that both CD44 and RGD have been shown previously to stimulate migration on 2D surfaces (within specific ranges of ligand density), our results suggest that the effect of adhesive ligands on cell migration depends strongly on the geometry in which these ligands are presented [41], consistent with previous reports that have shown that receptor-ligand interactions may be strongly affected by affixation to a solid-state scaffold [33,42].

We hypothesize that dorsal adhesion, whether mediated by CD44 or integrins, effectively serves as a drag force that retards efficient cell migration, such that increased dorsal adhesion progressively slows migration. Inhibition of myosin II or its activators ROCK and MLCK strongly reduces the ability of dorsal adhesions to slow motility, supporting a model in which myosin II links adhesive signals generated at the ventral surface to adhesive events at the dorsal surface (Figure 8). Our adhesion strength measurements reveal that myosin II increases the strength of not only integrin-RGD adhesions, as has been reported previously [34], but also the strength of CD44-HA adhesions. In this manner, ventral cues influence dorsal adhesions: integrin ligation and complex formation at the ventral surface would be expected to enhance myosin II activation, which in turn reinforces dorsal adhesions and retards cell migration. Importantly, myosin II has been found to play a major role in multiple modes of both 3D cell migration [6,43,44], and it is possible that the dorsoventral crosstalk observed here may play unappreciated but important roles in those geometries as well. Our results would suggest that such crosstalk could be compatible with a variety of matrix ligand systems.

Finally, our results broadly suggest that the route of invasion in GBM may be partially dictated by a competitive balance between the adhesion at the dorsal and ventral surfaces of cells at tissue interfaces, such that strong adhesion to the vascular basement membrane promotes efficient perivascular migration. In intracranial xenograft models of GBM, increased cell attachment to type I and IV collagen is correlated with increased invasion along the perivascular spaces [45], and suppression of the collagen ligand integrin β1 is sufficient to block diffuse infiltration [46]. Indeed, an α_v integrin-inhibitory peptide directed against endothelial cells has extended progression-free survival in phase II clinical trials, and while phase III results with this agent have been considerably less promising [47,48], this raises optimism for the success of analogous agents directed against tumor cell-matrix interactions. Interfacial culture paradigms such as ours should facilitate mechanistic discovery and molecular screening in the development of these agents.

Conclusion

We have created a simple model system to recapitulate migration of GBM cells along vascular interfaces. By manipulating both adhesive receptors and matrix properties, we discovered that cells migrate most efficiently when adhesion to the dorsal surface is weak, whether that adhesion was mediated by CD44 or integrins. We anticipate that this paradigm could readily be adapted to other tumor systems and will facilitate deeper investigation into mechanisms through which these tumors infiltrate tissues.

Supplementary Material

Refer to Web version on PubMed Central for supplementary material.

Acknowledgments

This work was supported by awards from the NIH (1F32CA174361 to AR, 1DP2OD004213 and 1R21CA174573 to SK), an NSF/NCI Physical and Engineering Sciences in Oncology Award (CMMI 1105539 to SK), and the W. M. Keck Foundation.

References

1. Pathak A, Kumar S. Biophysical regulation of tumor cell invasion: moving beyond matrix stiffness. Integr Biol. 2011; 3(4):267–278.
2. Sahai E, Marshall CJ. Differing modes of tumour cell invasion have distinct requirements for Rho/ROCK signalling and extracellular proteolysis. Nat Cell Biol. 2003; 5(8):711–719. [PubMed: 12844144]
3. Doyle AD, Wang FW, Matsumoto K, Yamada KM. One-dimensional topography underlies three-dimensional fibrillar cell migration. J Cell Biol. 2009; 184(4):481–490. [PubMed: 19221195]
4. Lauffenburger DA, Horwitz AF. Cell migration: a physically integrated molecular process. Cell. 1996; 84(3):359–369. [PubMed: 8608589]
5. Friedl P, Wolf K. Tumour-cell invasion and migration: diversity and escape mechanisms. Nat Rev Cancer. 2003; 3(5):362–374. [PubMed: 12724734]
6. Friedl P, Wolf K. Plasticity of cell migration: a multiscale tuning model. J Cell Biol. 2009; 188(1): 11–19. [PubMed: 19951899]
7. Tozluoğlu M, Tournier AL, Jenkins RP, Hooper S, Bates PA, Sahai E. Matrix geometry determines optimal cancer cell migration strategy and modulates response to interventions. Nat Cell Biol. 2013; 15(7):751–762. [PubMed: 23792690]
8. Petrie RJ, Gavara N, Chadwick RS, Yamada KM. Nonpolarized signaling reveals two distinct modes of 3D cell migration. J Cell Biol. 2012; 197(3):439–455. [PubMed: 22547408]
9. Condeelis J, Segall JE. Intravital imaging of cell movement in tumours. Nat Rev Cancer. 2003; 3(12):921–930. [PubMed: 14737122]
10. Friedl P, Alexander S. Cancer invasion and the microenvironment: plasticity and reciprocity. Cell. 2011; 147(5):992–1009. [PubMed: 22118458]
11. Alexander S, Koehl GE, Hirschberg M, Geissler EK, Friedl P. Dynamic imaging of cancer growth and invasion: a modified skin-fold chamber model. Histochem Cell Biol. 2008; 130(6):1147–1154. [PubMed: 18987875]
12. G.Gritsenko P, Ilina O, Friedl P. Interstitial guidance of cancer invasion. J Pathol. 2012; 226(2): 185–199. [PubMed: 22006671]
13. Wolf K, Alexander S, Schacht V, Coussens LM, von Andrian UH, van Rheenen J, et al. Collagen-based cell migration models in vitro and in vivo. Semin Cell Dev Biol. 2009; 20(8):931–941. [PubMed: 19682592]
14. Agnihotri S, Burrell KE, Wolf A, Jalali S, Hawkins C, Rutka JT, et al. Glioblastoma, a brief review of history, molecular genetics, animal models and novel therapeutic strategies. Arch Immunol Ther Exp. 2013; 61(1):25–41.
15. Bernstein JJ, Woodard CA. Glioblastoma cells do not intravasate into blood vessels. Neurosurgery. 1995; 36(1):124–132. [PubMed: 7708148]
16. Scherer HJ. The forms of growth in gliomas and their practical significance. Brain. 1940; 63(1):1–35.
17. Laurent TC, Fraser JR. Hyaluronan. FASEB J. 1992; 6(7):2397–2404. [PubMed: 1563592]
18. Toole BP. Hyaluronan: from extracellular glue to pericellular cue. Nat Rev Cancer. 2004; 4(7): 528–539. [PubMed: 15229478]
19. O'Rourke MF, Staessen JA, Vlachopoulos C, Duprez D, Plante GE. Clinical applications of arterial stiffness; definitions and reference values. Am J Hypertens. 2002; 15(5):426–444. [PubMed: 12022246]
20. Levental I, Georges PC, Janmey PA. Soft biological materials and their impact on cell function. Soft Matter. 2012; 3:299–306.
21. Xiaoming, Zhang; Kinnick, RR.; Fatemi, M.; Greenleaf, JF. Noninvasive method for estimation of complex elastic modulus of arterial vessels. IEEE Trans Ultrason Ferroelectr Freq Control. 2005; 52(4):642–652. [PubMed: 16060513]
22. Ananthanarayanan B, Kim Y, Kumar S. Elucidating the mechanobiology of malignant brain tumors using a brain matrix-mimetic hyaluronic acid hydrogel platform. Biomaterials. 2011; 32(31):7913–7923. [PubMed: 21820737]

23. Ulrich TA, de Juan Pardo EM, Kumar S. The mechanical rigidity of the extracellular matrix regulates the structure, motility, and proliferation of glioma cells. Cancer Res. 2009; 69(10):4167–4174. [PubMed: 19435897]
24. Marklein RA, Burdick JA. Spatially controlled hydrogel mechanics to modulate stem cell interactions. Soft Matter. 2010; 6:136–143.
25. Torsvik A, Røsland GV, Svendsen A, Molven A, Immervoll H, McCormack E, et al. Spontaneous malignant transformation of human mesenchymal stem cells reflects cross-contamination: putting the research field on track - letter. Cancer Res. 2010; 70(15):6393–6396. [PubMed: 20631079]
26. Kim Y, Kumar S. CD44-mediated Adhesion to hyaluronic acid contributes to mechanosensing and invasive motility. Mol Cancer Res. 2014 In press.
27. Wang YL, Pelham RJ Jr. Preparation of a flexible, porous polyacrylamide substrate for mechanical studies of cultured cells. Meth Enzymol. 1998; 298:489–496. [PubMed: 9751904]
28. Rehfeldt F, Brown AEX, Raab M, Cai S, Zajac AL, Zemel A, et al. Hyaluronic acid matrices show matrix stiffness in 2D and 3D dictates cytoskeletal order and myosin-II phosphorylation within stem cells. Integr Biol. 2012; 4(4):422–430.
29. Ponta H, Sherman L, Herrlich PA. CD44: from adhesion molecules to signalling regulators. Nat Rev Mol Cell Biol. 2003; 4(1):33–45. [PubMed: 12511867]
30. Pietras A, Katz AM, Ekström EJ, Wee B, Halliday JJ, Pitter KL, et al. Osteopontin-CD44 signaling in the glioma perivascular niche enhances cancer stem cell phenotypes and promotes aggressive tumor growth. Cell Stem Cell. 2014; 14(3):357–369. [PubMed: 24607407]
31. Bourdon MA, Ruoslahti E. Tenascin mediates cell attachment through an RGD-dependent receptor. J Cell Biol. 1989; 108(3):1149–1155. [PubMed: 2466038]
32. Castellani P, Dorcaratto A, Siri A, Zardi L, Viale GL. Tenascin distribution in human brain tumours. Acta Neurochir. 1995; 136(1–2):44–50. [PubMed: 8748826]
33. Beningo KA, Dembo M, Wang Y. Responses of fibroblasts to anchorage of dorsal extracellular matrix receptors. Proc Natl Acad Sci USA. 2004; 101(52):18024–18029. [PubMed: 15601776]
34. Kuo J-C, Han X, Hsiao C-T, Yates Iii JR, Waterman CM. Analysis of the myosin-II-responsive focal adhesion proteome reveals a role for β-Pix in negative regulation of focal adhesion maturation. Nat Cell Biol. 2011; 13(4):383–393. [PubMed: 21423176]
35. Pasapera AM, Schneider IC, Rericha E, Schlaepfer DD, Waterman CM. Myosin II activity regulates vinculin recruitment to focal adhesions through FAK-mediated paxillin phosphorylation. J Cell Biol. 2010; 188(6):877–890. [PubMed: 20308429]
36. Oakes PW, Beckham Y, Stricker J, Gardel ML. Tension is required but not sufficient for focal adhesion maturation without a stress fiber template. J Cell Biol. 2012; 196(3):363–374. [PubMed: 22291038]
37. Han SJ, Bielawski KS, Ting LH, Rodriguez ML, Sniadecki NJ. Decoupling substrate stiffness, spread area, and micropost density: a close spatial relationship between traction forces and focal adhesions. Biophys J. 2012; 103(4):640–648. [PubMed: 22947925]
38. Solon J, Levental I, Sengupta K, Georges PC, Janmey PA. Fibroblast adaptation and stiffness matching to soft elastic substrates. Biophys J. 2007; 93(12):4453–4461. [PubMed: 18045965]
39. Sen S, Dong MM, Kumar S. Isoform-specific contributions of alpha-actinin to glioma cell mechanobiology. PloS One. 2009; 4(12):e8427. [PubMed: 20037648]
40. Keung AJ, de Juan-Pardo EM, Schaffer DV, Kumar S. Rho GTPases mediate the mechanosensitive lineage commitment of neural stem cells. Stem Cells. 2011; 29(11):1886–1897. [PubMed: 21956892]
41. Ariza A, López D, Mate JL, Isamat M, Musulén E, Pujol M, et al. Role of CD44 in the invasiveness of glioblastoma multiforme and the noninvasiveness of meningioma: an immunohistochemistry study. Hum Pathol. 1995; 26(10):1144–1147. [PubMed: 7557949]
42. Mehta G, Williams CM, Alvarez L, Lesniewski M, Kamm RD, Griffith LG. Synergistic effects of tethered growth factors and adhesion ligands on DNA synthesis and function of primary hepatocytes cultured on soft synthetic hydrogels. Biomaterials. 2010; 31(17):4657–4671. [PubMed: 20304480]

43. Poincloux R, Collin O, Lizárraga F, Romao M, Debray M, Piel M, et al. Contractility of the cell rear drives invasion of breast tumor cells in 3D Matrigel. Proc Natl Acad Sci USA. 2011; 108(5): 1943–1948. [PubMed: 21245302]

44. Wolf K, Friedl P. Molecular mechanisms of cancer cell invasion and plasticity. Br J Dermatol. 2006; 154(1):11–15. [PubMed: 16712711]

45. Piao Y, Lu L, de Groot J. AMPA receptors promote perivascular glioma invasion via ?1 integrin-dependent adhesion to the extracellular matrix. Neuro Oncol. 2009; 11(3):260–273. [PubMed: 18957620]

46. Paulus W, Baur I, Beutler AS, Reeves SA. Diffuse brain invasion of glioma cells requires beta 1 integrins. Lab Invest. 1996; 75(6):819–826. [PubMed: 8973477]

47. Reardon DA, Zalutsky MR, Akabani G, Coleman RE, Friedman AH, Herndon JE 2nd, et al. A pilot study; 131I-antitenascin monoclonal antibody 81c6 to deliver a 44-Gy resection cavity boost. Neuro Oncol. 2008; 10(2):182–189. [PubMed: 18287339]

48. Stupp R, Hegi ME, Gorlia T, Erridge S, Grujicic D, Steinbach JP, et al. Cilengitide combined with standard treatment for patients with newly diagnosed glioblastoma and methylated O6-methylguanine-DNA methyltransferase (MGMT) gene promoter: Key results of the multicenter, randomized, open-label, controlled, phase III CENTRIC study. J Clin Oncol. 2013; 31

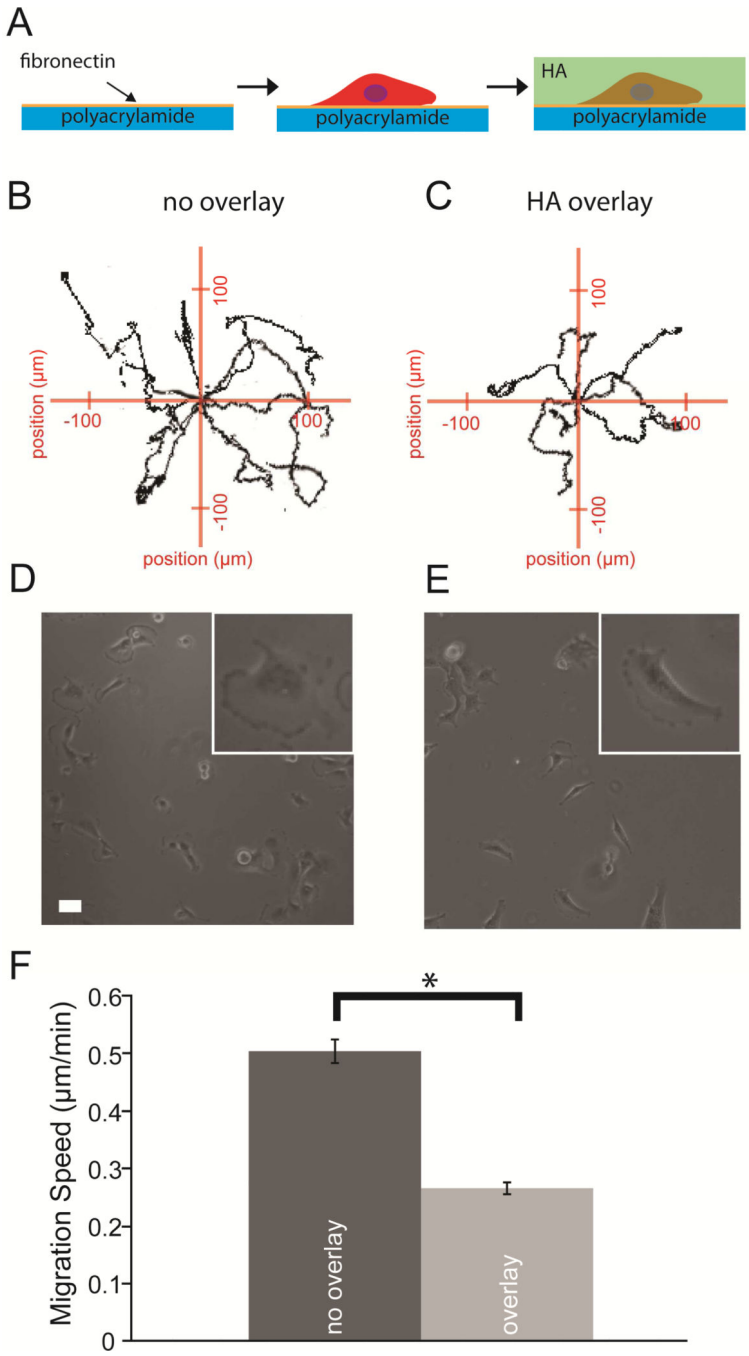

Figure 1.

Effects of HA overlay on cell migration. (A) Schematic of system. Initially, cells are seeded on defined-stiffness polyacrylamide hydrogels. After cell adhesion and spreading, soluble methacrylate-modified HA is cross-linked with DTT to form an insoluble network around the dorsolateral aspect of the cells. (B, C) Representative trajectories of single migrating cells over a 5 hr. period on a ventral fibronectin-coated polyacrylamide surface without (B) or with (C) a dorsal HA overlay present. (D, E) Phase contrast images of cells in these two configurations. (F) Quantification of migration speed under each condition. N=131, 125

cells for overlay and no overlay, respectively. *P<0.05. Error bars are S.E.M. Scale bar is 50 μm.

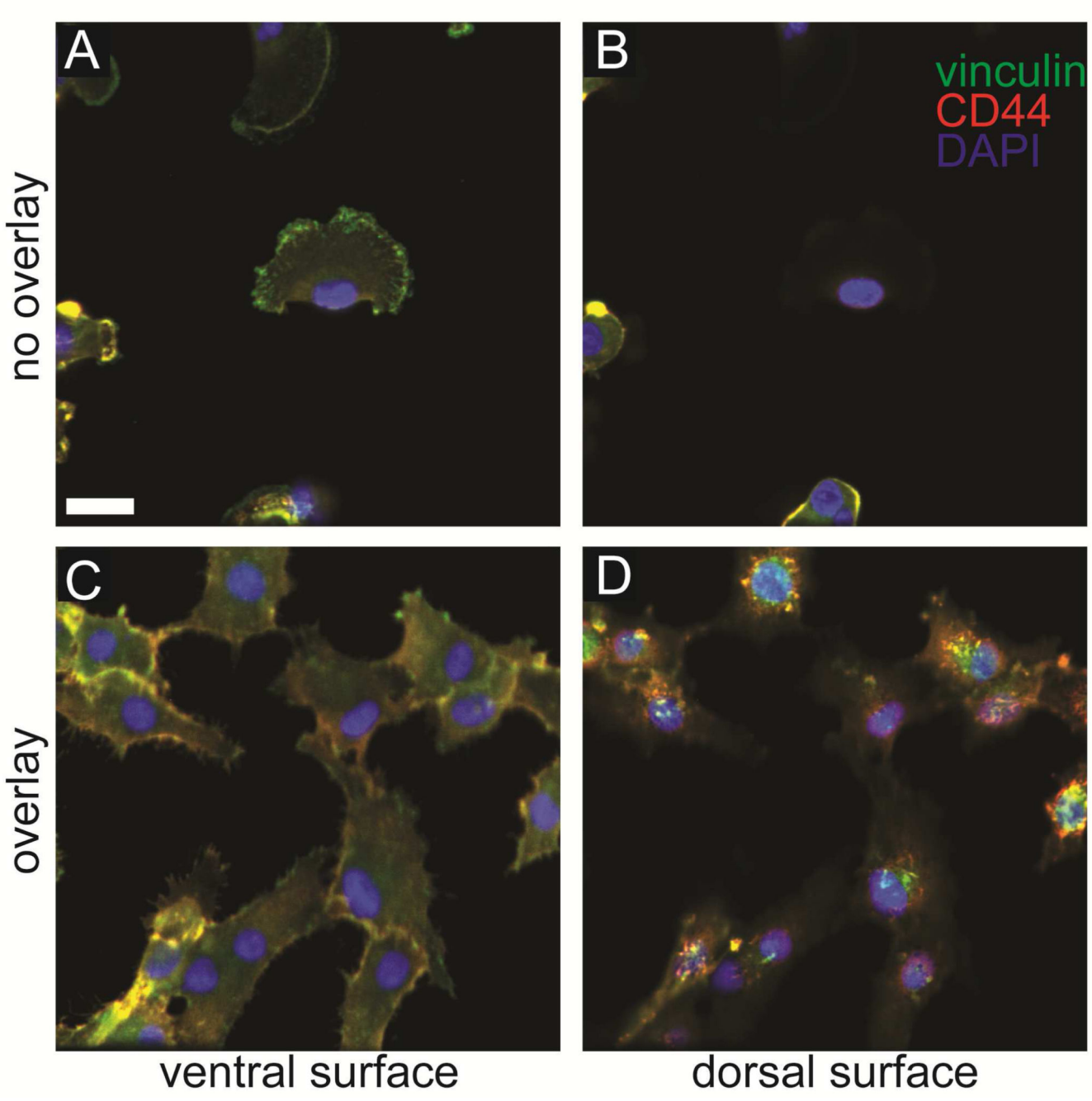

Figure 2.

Vinculin and CD44 localization in overlay cultures. (A, C) Immunostained U373-MG cells in control and overlay cultures stained for the focal adhesion marker vinculin, and HA-receptor CD44 and imaged at the ventral surface. (B, D) Similarly stained cells imaged at the dorsal surface. Scale bar, 25 μm.

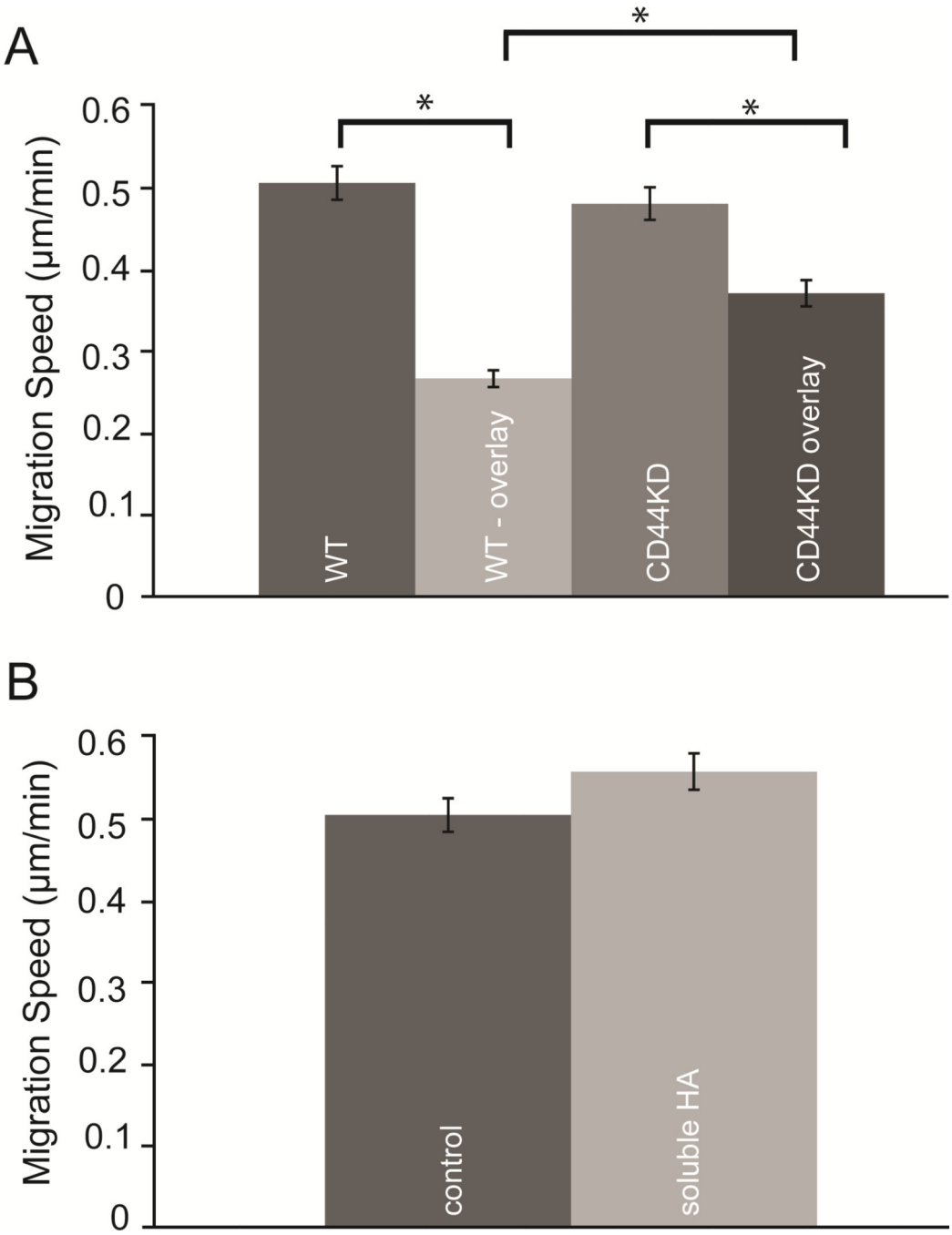

Figure 3.

Effects of CD44 ligation on migration reduction in overlay cultures. (A) Migration speed of CD44 knockdown and control cells in both overlay and 2D configurations. (B) Migration speed of cells with and without the addition of 0.375 mg/ml soluble HA on polyacrylamide surfaces. N=131, 125 cells for wild-type overlay and no overlay, respectively. N=153, 135 cells for CD44KD overlay and no overlay, respectively. *=$p<0.05$. Error bars are S.E.M.

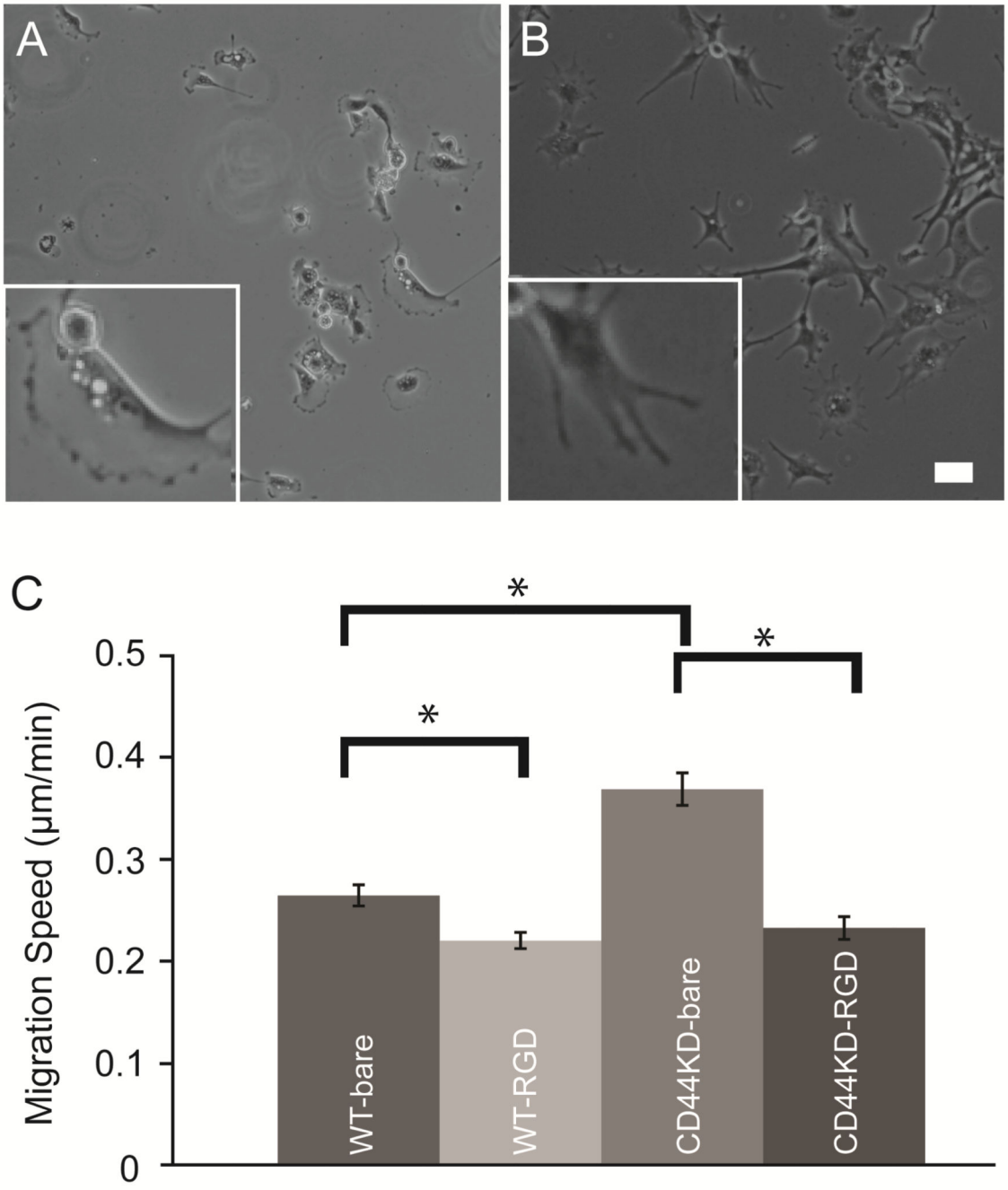

Figure 4.

Migration reduction via inclusion of additional adhesive domains. Phase contrast images of cells in (A) bare hyaluronic acid overlays and (B) overlays conjugated with 1 mM integrin-adhesive RGD domains via Michael addition chemistry. (C) Migration speed for wild-type cells with bare HA and RGD-HA matrices, as well as CD44 KD cells with bare HA and RGD-HA matrices. N=125, 101 cells for wild-type bare HA and RGD-HA, respectively. N=135, 96 cells for CD44KD bare HA and RGD-HA, respectively. *=$p<0.05$. Error bars are S.E.M. Scalre bar, 25 microns.

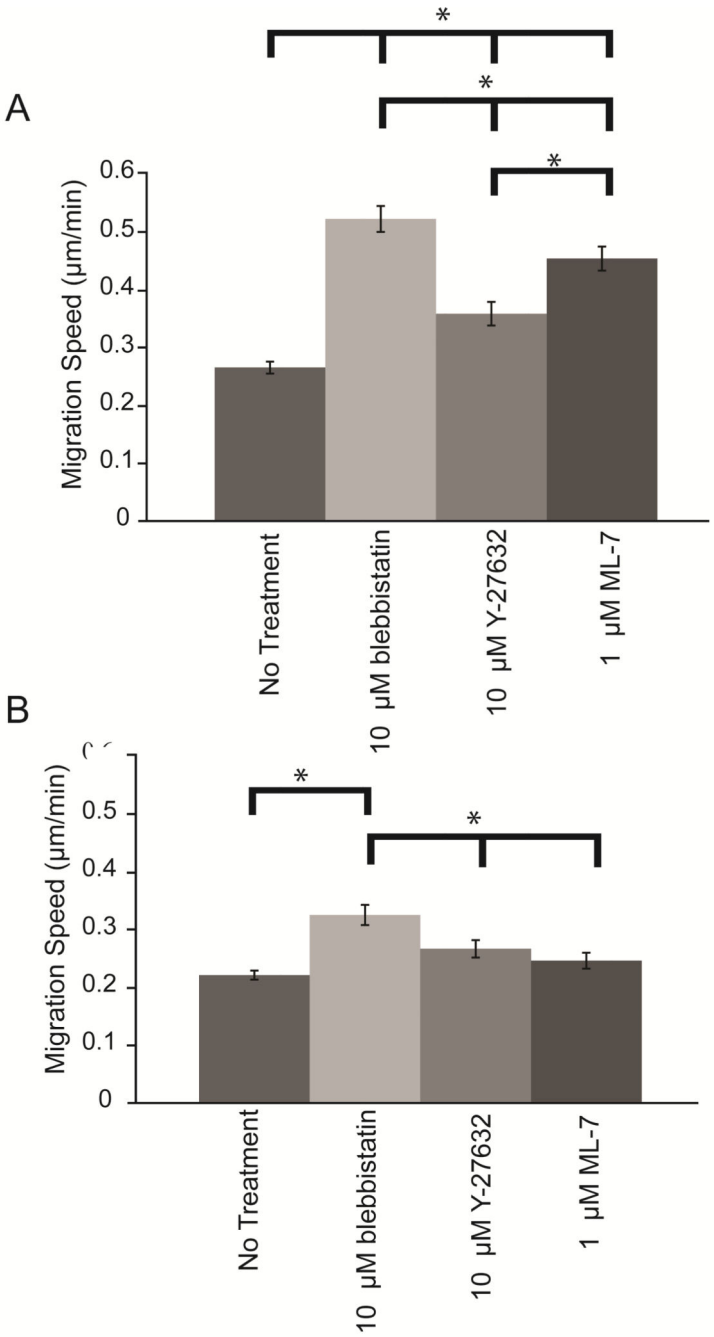

Figure 5.

Role of contractility in overlay-induced migration reduction. Migration speed of U373-MG cells with the addition of 10 uM blebbistation, 10 uM Y-27632, or 1 uM ML-7 in either (A) bare-HA or (B) RGD-HA overlays. N= 131, 88, 90, 94 for bare HA control, blebbistatin, Y-27, and ML-7, respectively. N= 125, 91, 98, 94 for RGD-HA control, blebbistatin, Y-27, and ML-7, respectively. *=$p<0.05$. Error bars are S.E.M.

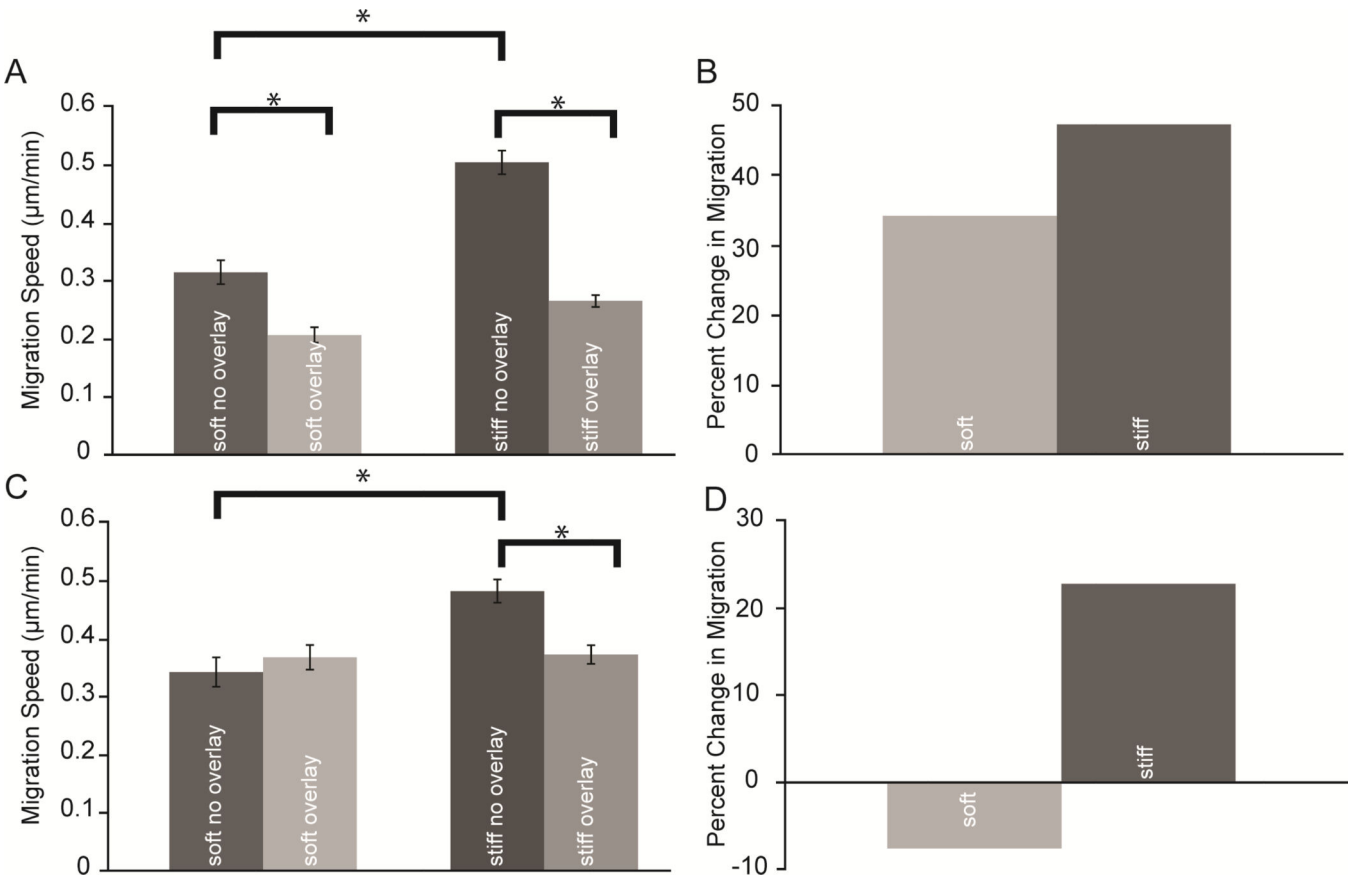

Figure 6.

Effects of ventral surface stiffness on cellular response to HA overlay. (A) U373-MG cell migration speed in bare-HA overlays after varying the stiffness of the dorsal polyacrylamide layer by altering the cross-linking ratio of the acrylamide solution. (B) Relative difference in migration speed calculated as the percent change in migration speed between the control and bare-HA overlay case. (C, D) Previous experimental paradigm repeated with CD44KD cells. N= 82, 54, 130, 125 for U373-MG cells on soft polyacrylamide no overlay, soft polyacrylamide overlay, stiff polyacrylamide no overlay, and stiff polyacrylamide overlay, respectively. N= 89, 40, 152, 134 for CD44KD cells on soft polyacrylamide no overlay, soft polyacrylamide overlay, stiff polyacrylamide no overlay, and stiff polyacrylamide overlay, respectively.*=$p<0.05$. Error bars are S.E.M.

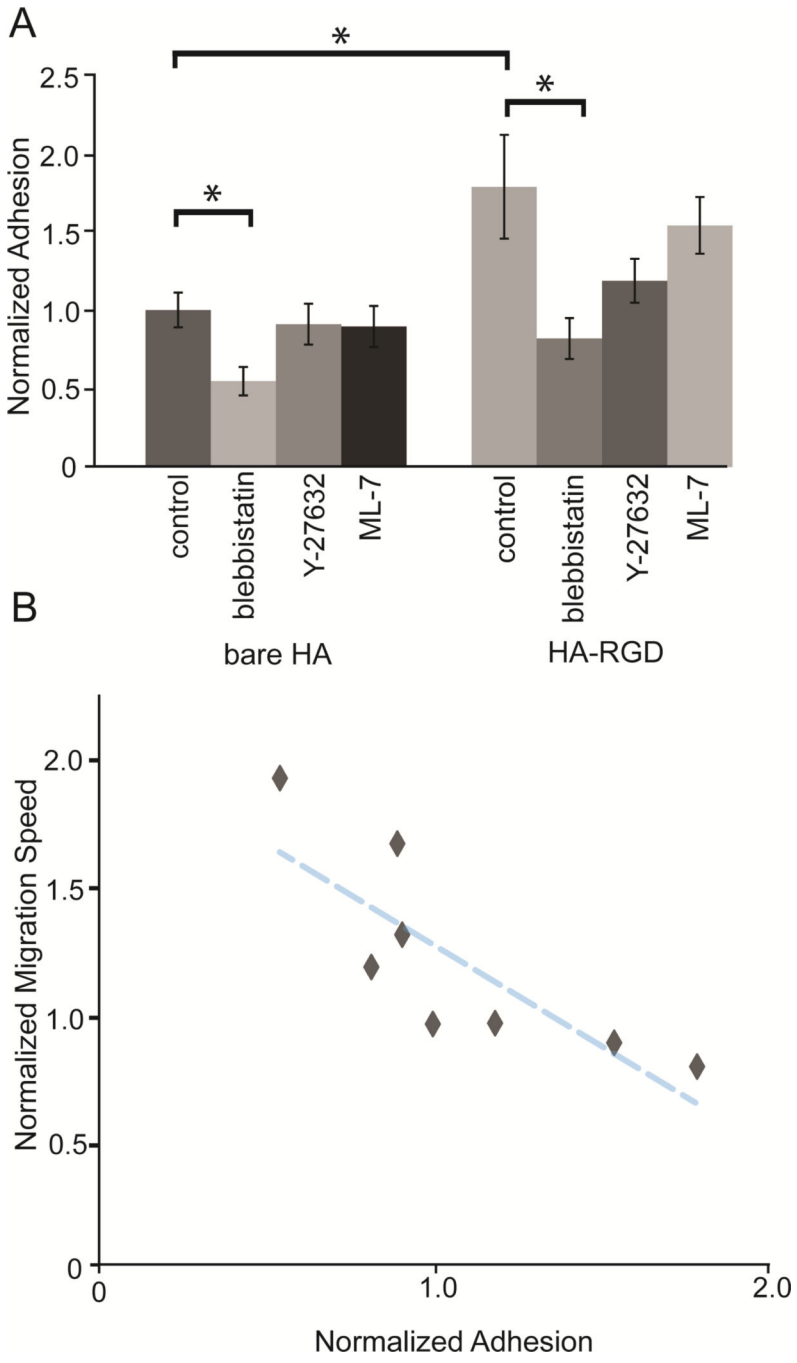

Figure 7.

Correlation of dorsal adhesivity with migration speed in overlay cultures. (A) Normalized number of cells remaining on 2D gel after centrifugation at 100g for 5 min. (B) Normalized adhesive strength plotted against the migration speed of each overlay condition normalized to the bare-HA overlay control migration, overlaid with a linear best-fit curve (R^2=0.66). N= 17, 17, 11, 12 experiments for bare HA control, blebbistatin, Y-27, and ML-7, respectively. N= 10, 9, 23, 22 for RGD-HA control, blebbistatin, Y-27, and ML-7, respectively. *=p<0.05. Error bars are S.E.M.

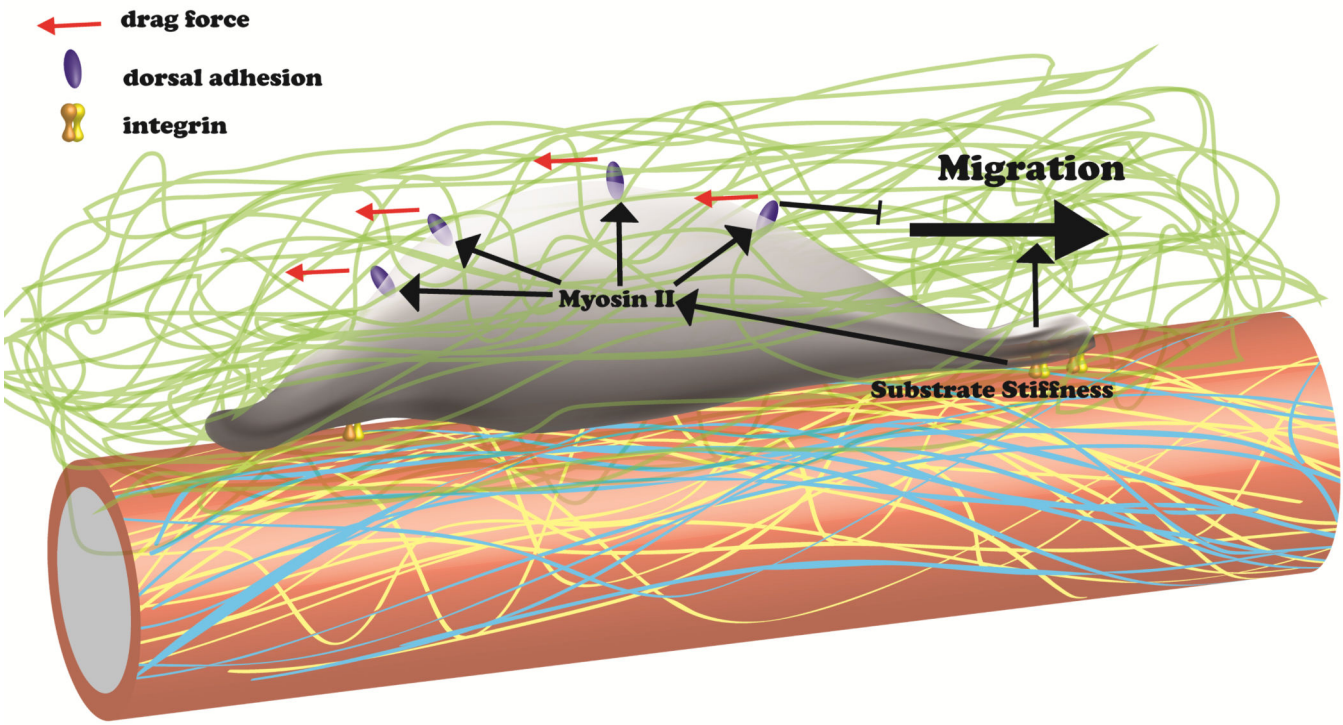

Figure 8.

Integrated model of cell migration through interfaces. Membrane-spanning integrins (yellow and orange) partially interpret the biochemical and biophysical properties of the basolateral membrane of vessels (blue and yellow lines). Activation of integrins results in increased myosin II activity, which increases dorsal adhesions (purple ovals) resulting in increased drag forces (red arrows) that hinder efficient forward migration.